



## **Integrated spiral inductor with substrate silicon in a buck converter**

Abdelhadi Namoune<sup>a,\*</sup>, Rachid Taleb<sup>b</sup>

<sup>a</sup> *Electrical Engineering Department, Ahmed Zabana University Centre, Relizane, Algeria*

<sup>b</sup> *Electrical Engineering Department, Hassiba Benbouali University, LGEER Laboratory, Chlef, Algeria*

---

### ARTICLE INFO

#### Article history:

Received 14 August 2020

Accepted 15 October 2020

#### Keywords:

Buck converter

Integration

Spiral inductor

Geometric parameters

Substrate

---

### ABSTRACT

In this paper, we discuss the design and modelling of a spiral inductor with silicon substrate. The equivalent electrical model approved of the integrated spiral inductor acquires into account the inductance and quality factor. The performance of the inductance and quality factor values is supported on the mathematical study of the effect geometrical elements on the spiral inductor. The results simulation based on the MATLAB software. Finally, is discussing after simulation about the integrated spiral inductor into a DC-DC converter by PSIM 6.0.

---

## 1. Introduction

Inductors are essential components for radio frequency communication devices. A typical device such as a cell phone may utilize more than 20 inductors [1]. In 2012 alone, over 1.7 billion mobile phones were sold [2], and that number is only expected to increase. With the evolution of technology, there is an ever-increasing demand for communication devices with

---

\* Corresponding author, E-mail address: [namoune.abdelhadi@gmail.com](mailto:namoune.abdelhadi@gmail.com)

Tel.: +213 771795748

ISSN: 1112-2242 / EISSN: 2716-8247



This work is licensed under a Creative Commons Attribution-ShareAlike 4.0 International License.

Based on a work at <http://revue.cder.dz>.

improved signal quality and reception, reduced power consumption, and smaller packaging. To accomplish these goals, it is critical to integrate high-quality passive components, but unfortunately, available on-chip inductors traditionally exhibit poor performance. Designers are thus faced with suffering the low quality of on-chip devices, or they must resort to larger off-chip inductors that come with an increase in power consumption, cost, and area [3]. Divers papers have been devoted to integrated inductors through silicon substrates used in power change [4-7].

A number of reasons form of losses that influence the behavior of the inductors [8]. Practical archetypes require to be constructed before manufacturing, in order to decrease the fabricating cost and to augment the dependability of the planned circuits. Design and modeling are important in studying integrated inductors with silicon for power change [9-10].

The initial element of the work illustrates the design and modeling method of integrated inductors with substrate. The next element discusses the behavior of the inductor in a universal advance tending nears the complete integration of petite power systems such as those designed for portable phones. Then, the effect of different geometrical elements such as the working frequency, the number of turns, the width of metal trace and the space between turns are examined in simulations by MATLAB. Lastly, an application by the integrated inductor in a buck converter illustrated.

## **2. Design and modelling spiral inductor**

The basic structure of an integrated inductor is made up of one or more metal tracks in parallel forming one or several concentric turns, requiring a minimum of two metal layers and one via connection between them for inductors with 2 or more turns. In order to design an inductor it is important to consider both the vertical and lateral geometries of the layout. In Figure 1 it is possible to observe a three dimensional square spiral inductor.

Square spirals are popular due to its easy layout. However, some other layouts can be used to improve the inductor performance. Layouts such as hexagonal and octagonal have already been reported. If desired, a circular layout may be approximated using a polygonal with many sides. Figure 2 shows the different layouts, for square, hexagonal and octagonal respectively [12].

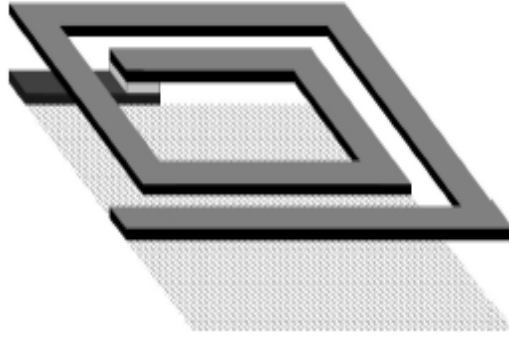


Fig. 1: 3-D view of a square spiral inductor [11].

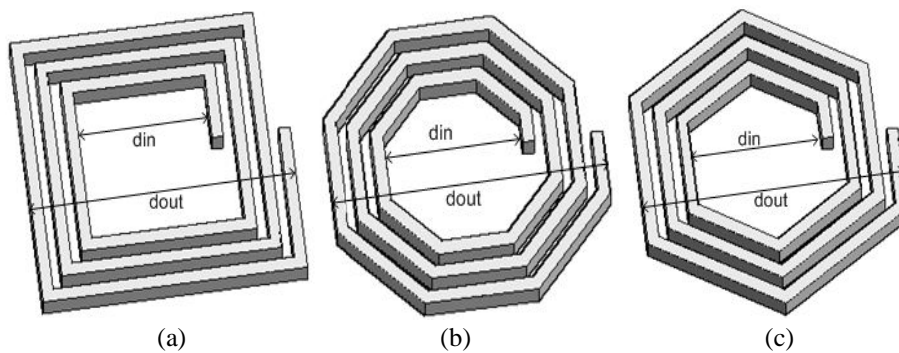


Fig. 2. Different implementations of inductor (a) square, (b) octagonal, (c) hexagonal

The geometry of a planar spiral inductor is defined by five geometric parameters:

1. number of turns,  $n$ ,
2. metal width,  $w$ ,
3. spacing between turns,  $s$ ,
4. the outer diameter,  $d_{out}$ ,
5. the inner diameter,  $d_{in}$ .

The average diameter ( $d_{avg}$ ). The fill ratio ( $\rho$ ) is given by either of the following expressions [13]

$$\rho = \frac{d_{out} - d_{in}}{d_{out} + d_{in}} \quad (1)$$

The most important performance characteristics for spiral-integrated inductors are the inductance ( $L$ ) and the quality factor ( $Q$ ). The five geometric parameters presented are responsible for the definition of inductance. However,

Figure 3 illustrates the conventional  $\pi$ -type model describing the impedance behavior of a two-port inductor on a lossy substrate. The elements constituting the equivalent model are indicated in the schematic cross-section of a planar spiral inductor represented in Figure 4. The physical meaning of the lumped elements is the following [14] :  $L_s$  and  $R_s$  represent the series inductance and series resistance of the metal trace (i.e., spiral and underpass). The term  $C_s$  models the capacitive coupling due to the overlap between the spiral and the underpass.

The network composed by  $C_{ox}$ ,  $R_{sub}$  and  $C_{sub}$  accounts for the parasitics associated to the lossy substrate.  $C_{ox}$  models the oxide capacitance between the spiral and the substrate; whereas,  $R_{sub}$  and  $C_{sub}$  represent the silicon substrate resistance and capacitance, respectively [15].

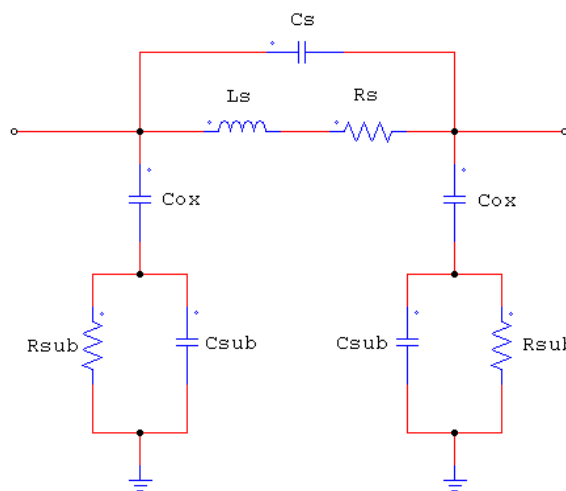


Fig. 3. Conventional  $\pi$ -type equivalent model representing a two-port inductor on a lossy substrate.

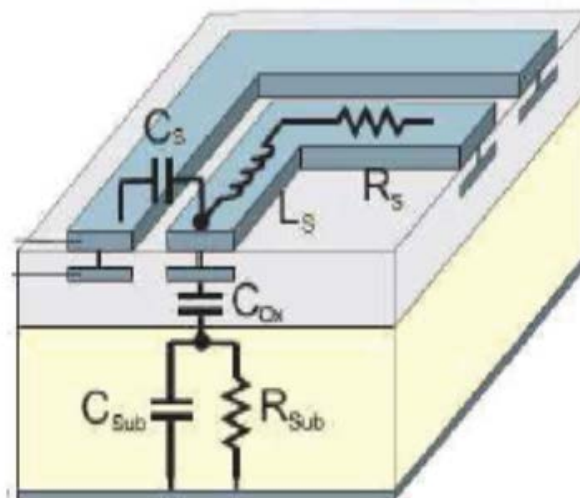


Fig. 4. Schematic cross-section of a two-port spiral inductor on a lossy substrate.

The inductance ( $L_s$ ) calculation of each coil is determined by approximate expressions derived in [16]. The equation for the series inductance is [16] :

$$L_s = \frac{2\mu n^2 d_{avg}}{\pi} \left[ \ln\left(\frac{2,067}{\rho}\right) + 0,178 \cdot \rho + 0,125 \cdot \rho^2 \right] \quad (2)$$

Where  $\mu$  is the magnetic permeability of free space ( $\mu=4\pi \cdot 10^{-7}$  H/m),  $n$  is the number of turns of the coil,  $d_{avg}$  is the average diameter of the turns, and  $\rho$  is the fill ratio [17].

The series resistance is calculated by the following equation:

$$R_s = \frac{l}{\sigma \delta w (1 - e^{-t/\delta})} \quad (3)$$

Where  $l$  and  $w$  are the length and width of the spiral,  $\sigma$  is the metal conductivity,  $t$  is the metal thickness, and  $\delta$  is the skin length given by [18]:

$$\delta = \sqrt{\frac{2}{2\pi f \cdot \mu \sigma}} \quad (4)$$

Where  $f$  is the frequency. The series resistance expression models the increase of resistance at higher frequencies due to the skin effect [19].

For the evaluation of the capacitance,  $C_s$ , all overlap capacitances are considered and given by [20].

$$C_s = \frac{nw^2 \varepsilon_{ox}}{t_{ox}} \quad (5)$$

Where  $\varepsilon_{ox}$  is the oxide permittivity and  $t_{ox}$  is the oxide thickness between the spiral upper and lower metal. The parasitic capacitance,  $C_{ox}$ , between the spiral metal and the silicon substrate, is estimated with [20]

$$C_{ox} = \frac{0,5lw\varepsilon_{ox}}{t_{ox}} \quad (6)$$

Finally the Substrate resistance,  $R_{sub}$ , and capacitance  $C_{sub}$ , are obtained with [20]

$$R_{sub} = \frac{2h_{sub}}{lw\sigma_{sub}} \quad (7)$$

$$C_{sub} = \frac{0,5lw\epsilon_0\epsilon_r}{h_{sub}} \quad (8)$$

Where  $\sigma_{sub}$  and  $h_{sub}$  are the substrate conductivity and height, respectively

The simulation process followed for the analysis of inductor is meshing and porting of the device. After porting S-parameters are obtained to calculate Quality factor and inductance. Now from S-parameters, Y Parameters are obtained. Using Y-Parameters the quality factor and inductance values are calculated using the expressions shown in Equation (9) and Equation (10) respectively [21-22]:

$$L = \frac{Im\{Y_{11}\}^{-1}}{2\pi.f} \quad (9)$$

$$Q = \frac{Im\{Y_{11}\}^{-1}}{Re\{Y_{11}\}^{-1}} \quad (10)$$

Where,  $f$  represents the frequency.  $L$ ,  $Q$ ,  $Y$  represent the inductance, quality factor and admittance respectively. The symbol  $Im$  and  $Re$  represents the imaginary part and real part respectively.

Variable geometrical parameter of spiral inductor layout has been proposed as a way of maximizing the quality factor of integrated inductors. In this work, five spiral inductor designs have been created. The designs have the same dielectric layers and physical layout but of different geometry dimensions. All related variable parameters for these designs are shown in Table 1. Design 1 is set as the reference design.

Table 1. Design geometries of the square inductor

	dout ( $\mu\text{m}$ )	din ( $\mu\text{m}$ )	n	w ( $\mu\text{m}$ )	s ( $\mu\text{m}$ )
Design 1	182	70	3	14	7
Design 2	140	70	2	15,5	4
Design 3	140	70	2	14	7
Design 4	140	80	2	13	4
Design 5	120	60	2	12,5	5

### 3. Results and discussion

By using MATLAB simulation software, the characterization of spiral inductor permits more flexibility during the design process. The effect of spiral inductor geometry variations can be more easily analyzed.

#### 3.1 Effect on quality factor and inductance

##### 3.1.1 Design comparison

The effects on inductance and quality factor computed from equations (9 and 10) are shown in Figure 5 and Figure 6.

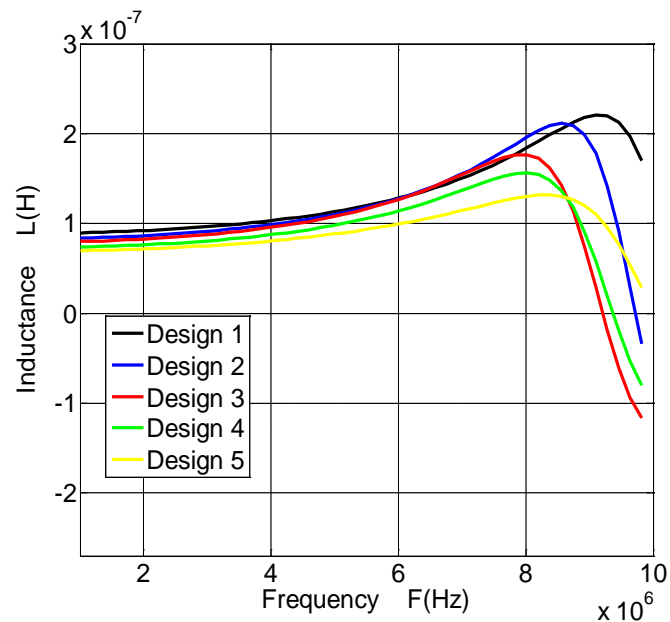


Fig. 5. Effect on inductance value, L for different designs of spiral inductor

Analysis from 1 MHz to 10 MHz was done to investigate the effects on inductance and quality factor. Design 1 produces the highest quality factor at 5 MHz. Compared to the others; Design 5 has the smallest dimension and also produces small inductance value. Design 2 is chosen as the basic design because this design fulfills the desired specifications such as quality factor more than 13.

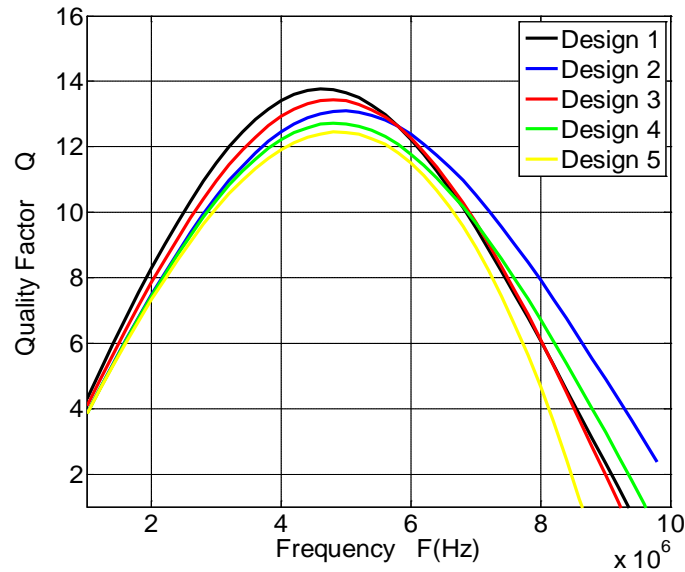


Fig. 6. Effect on quality factor for different design of spiral inductor

### 3.1.2 Number of turns

The first geometrical element is the number of turns of the spiral inductor. The  $L$  and  $Q$  for different values of number of turns (2, 3 and 4) are illustrating in Figures 7 and 8.

The inductance value augments when the spiral has additional turns. However, from Figure 7, we can infer that the inductance value does not augment linearly with the  $n$ , as the area of the inside diameter ( $d_{in}$ ) is lesser compare to the outer diameter. The self-resonance frequency diminishes importantly for every new winding added because of the augmented capacitive coupling among the substrate and the turns. The peak quality factor also diminishes significantly with augmenting number of turns because the augmented metal loss of the conductor.

### 3.1.3 Width of conductor

The width of the conductor influences the behavior of the spiral inductor to very large extent, as illustrate in Figures 9 and 10.

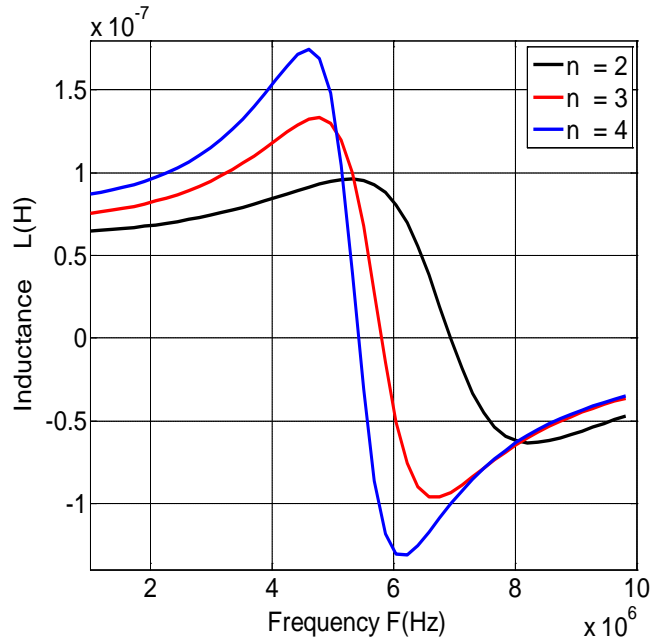


Fig. 7. Effect on inductance,  $L$  value for different number of turns

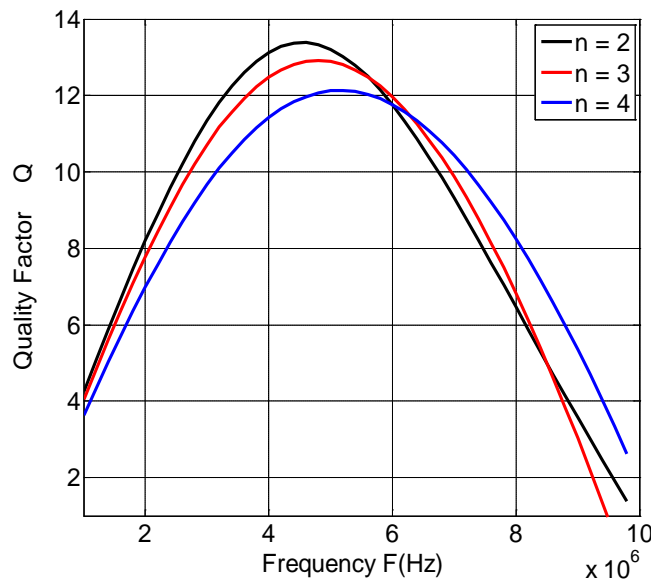


Fig. 8. Effect on quality factor,  $Q$  for different number of turns

The width of the metal trace is diverse from  $10\ \mu\text{m}$  to  $18\ \mu\text{m}$ . The  $L$  value diminishes as the ring region of the inside diameter ( $d_{in}$ ) reduces with growing width, but the self-resonance frequency diminishes because of the better capacitive coupling of the square inductor to the silicon. Since the series loss reduces with augmenting  $w$ , the  $Q$  quality factor enhances, but not linearly, in fact augmenting the width, which reduces the series resistance, only augments the peak  $Q$  from 12 to 13,2.

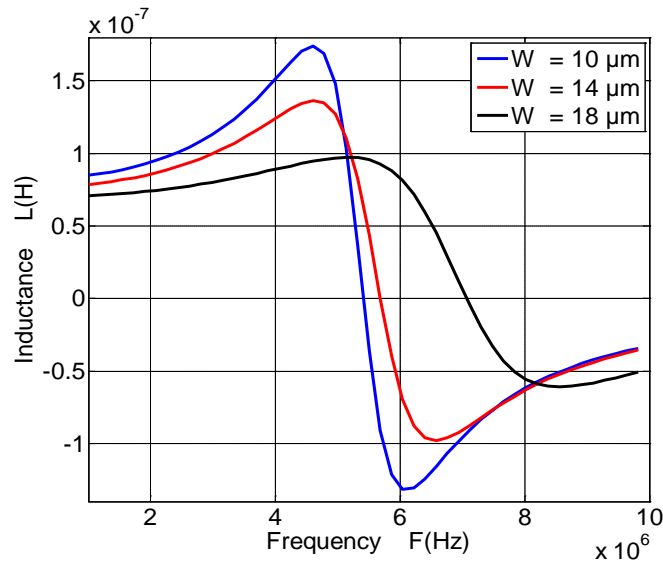


Fig. 9. Effect on inductance,  $L$  value for different width of conductor

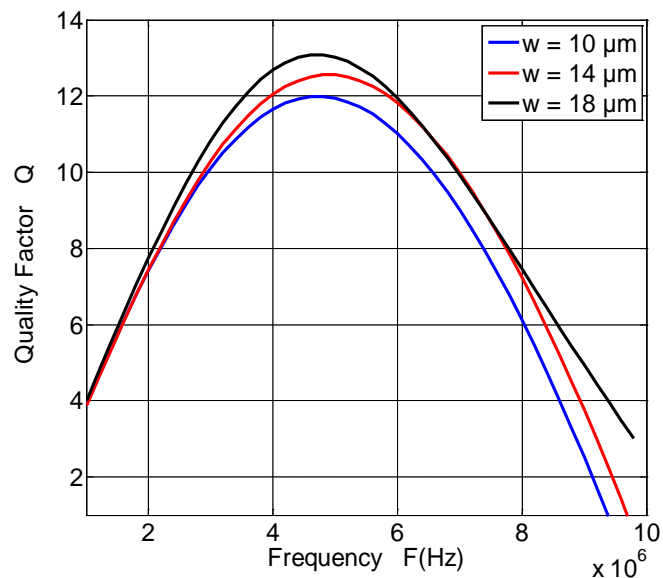


Fig. 10. Effect on quality factor,  $Q$  for different width of conductor

### 3.1.4 Space between turns

The separation distance between turns also changes the effective inductance value and quality factor. Metal spacing is varied from  $6 \mu m$  to  $10 \mu m$ . The simulation results are shown in Figures 11 and 12.

The inductance value decreases with increasing the distance between turns, as the ring region of the inside diameter ( $d_{in}$ ) spiral inductor diminishes with augmenting space between turns. Smaller space between turns results in superior capacitive coupling among the turns and

consequently a lower self-resonance frequency. The peak of the  $Q$  is not so responsive to the space between turns.

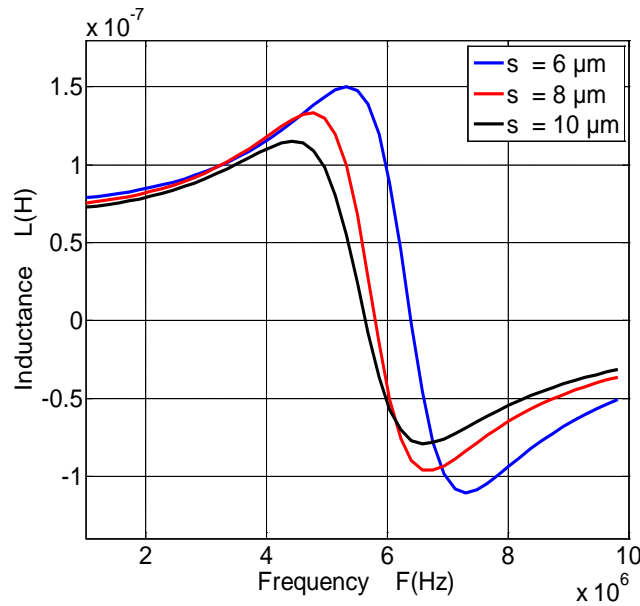


Fig. 11. Effect on inductance,  $L$  value for different space between turns

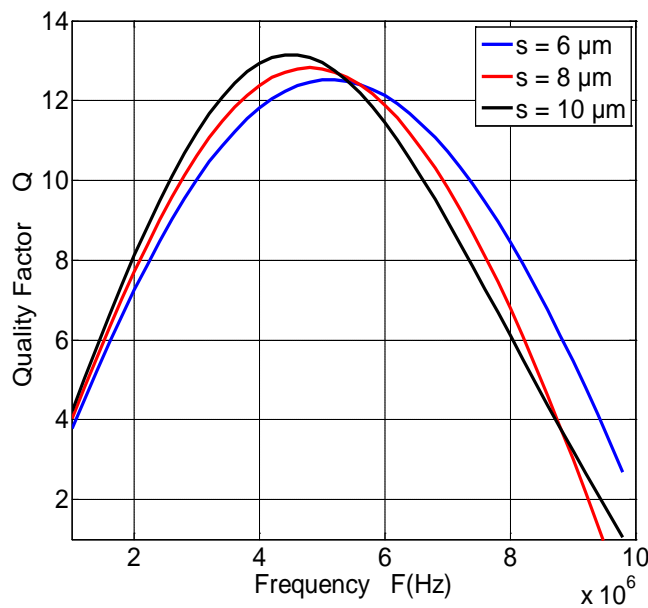


Fig. 12. Effect on quality factor,  $Q$  for different space between turns

### 3.2 Comparison with state of the art work

Comparison between previous works and my design is shown in Table 2. The values mentioned in the table under my work are the size of inductor, maximum quality factor and inductance

value obtained by the parametric analysis. The area of spiral inductor for the entire analysis process is same as mentioned.

Table 2. Comparison of different spiral inductors

Inductor design	Size ( $\mu\text{m}^2$ )	Q <sub>max</sub>	L (H)	Réf
Spiral inductor (Octagonal inductor)	140*140	12	$75 \cdot 10^{-9}$	[23]
Spiral inductor (Hexagonal inductor)	300*300	22	$33,3 \cdot 10^{-9}$	[24]
Spiral inductor (Square inductor)	180*160	13,3	$78 \cdot 10^{-9}$	My work

#### 4. Buck converter application

The circuit of the synchronous buck converter shown in Figure 13 is used to evaluate the performance of the integrated inductor. This topology of the converter is chosen because it provides better performance since it does not require an isolation transformer. The inductor we intend to integrate will be sized for this type of application. In the simulation we used PSIM software; the values of the micro converter electrical characteristics are enlisted in Table 3:

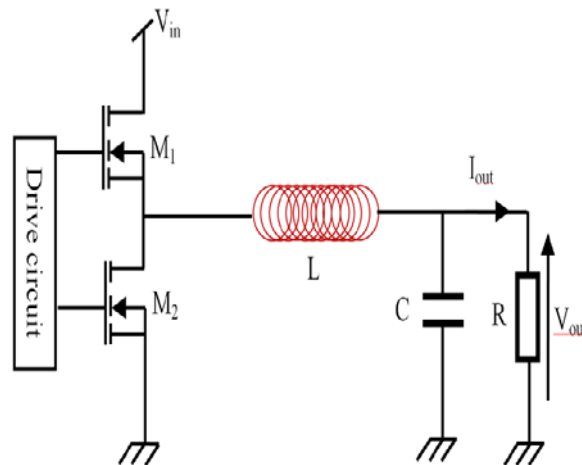


Fig. 13. Schematic diagram of Buck converter DC-DC

Table 3. Design specifications of buck micro converter DC-DC

Electrical characteristics	Symbol	Value
Input Voltage	V <sub>in</sub>	3,3 V
Output voltage	V <sub>out</sub>	1,5 V
Output current	I <sub>out</sub>	0,5
Switching frequency of the converter	f	5 MHz

Figure 14 shows the waveform of the output voltage and current of the Buck converter with integrated spiral inductor. The output current ( $I_{out}$ ) simulated at a switching frequency of 5 MHz is illustrate in red color. It is remarked that the ( $I_{out}$ ) is stable; the buck converter distributes an ( $I_{out}$ ) of about 0, 5 A. In addition, the output voltage ( $V_{out}$ ) is illustrated in blue color. It is also significant to observe that the input voltage ( $V_{in}$ ) of 3,3 V is lessened to 1,5 V.

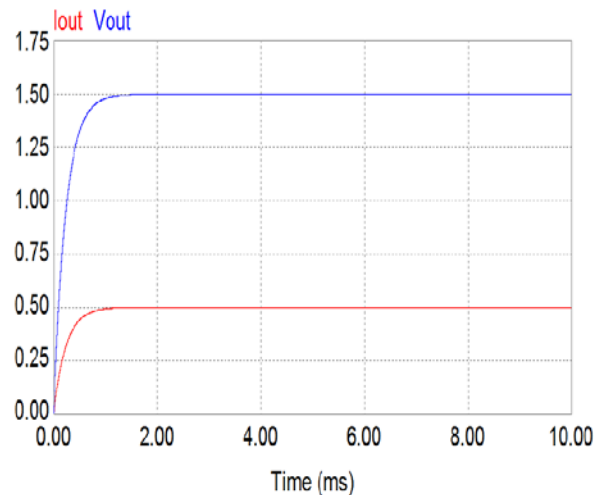


Fig. 14. Output voltage and current of the Buck converter with integrated spiral inductor

## 5. Conclusions

In this paper, we proposed an integrated inductor design process with a substrate. Using the developed procedure, we demonstrated that the value of the inductor and the quality factor of the inductor could be predicted prior to manufacturing. Then, the influence of various parameters such as the operating frequency, the space between the turns, the number of turns, and the width of conductor were analyzed in detail based on simulations using the MATLAB to determine the optimal geometrical parameters of the inductor. The efficiency study of the integrated inductor in an application of the energy conversion was established. The desired value of the output voltage was also obtained from the simulation of the DC-DC buck converter microwave. The results show that the developed structure of the inductor is a very promising approach for the monolithic integration of DC-DC converters.

## 6. References

- [1] Namoune, A., Hamid, A., & Taleb, R. (2017). The Performance of an Integrated Transformer in a DC/DC Converter. TELKOMNIKA (Telecommunication, Computing, Electronics and Control), 15(3), 1031–1039.

- [2] Wibben, J., & Harjani, Ramesh. (2008). A High-Efficiency DC–DC Converter Using 2 nH Integrated Inductors. *IEEE Journal of Solid-State Circuits*, 43(4), 844–854.
- [3] Namoune, A., Taleb, R., Belboula, A., & Chabni, F. (2017). Design and modeling of miniature on chip spiral inductor for DC-DC converter. *Journal of Advanced Research in Science and Technology*, 4(2), 568–573.
- [4] Musunuri, S., Chapman, P., Zou, J., & Liu, C. (2003). Inductor design for monolithic DC-DC converters. Presented at the IEEE 34th Annual Conference on Power Electronics Specialist, 2003. PESC '03., Acapulco, Mexico.
- [5] Namoune, A., Taleb, R., Derrouazin, A., Belboula, A., & Hamid, A. (2019). Integrated square shape inductor with magnetic core in a buck converter DC-DC. *Przeglad Elektrotechniczny*, 95(9), 57–61.
- [6] Flynn, D, Toon, A., & Desmulliez, M. P. (2005). Manufacture and characterisation of micro-engineered DC-DC power converter using UV-LIGA process. *Electronics Letters*, 41(24), 1351–1353.
- [7] Musunuri, S., Chapman, P.L, Jun, Z., & Chang, L. (2005). Design issues for monolithic DC-DC converters. *IEEE Transactions on Power Electronics*, 20(3), 639–649. <https://doi.org/10.1109/TPEL.2005.846527>
- [8] Burghartz, J., & Rejaei, B. (2003). On the design of RF spiral inductors on silicon. *IEEE Transactions on Electron Devices*, 50(3), 718–729.
- [9] Namoune, A., Taleb, R., & Mansour, N. (2020). Design and modeling of solenoid inductor integrated with FeNiCo in high frequency. *TELKOMNIKA (Telecommunication, Computing, Electronics and Control)*, 18(4), 1746–1753.
- [10] Namoune, A., Taleb, R., Derrouazin, A., & Belboula, Abdelkader. (2019). Integrated Solenoid Inductor with Magnetic Core in a Buck Converter. *Przeglad Elektrotechniczny*, 95(8), 92–95.
- [11] Wang, M., Batarseh, Issa, D. T. Ngo, Khai, & Xie, Huikai. (2007). Design and Fabrication of Integrated Power Inductor Based on Silicon Molding Technology. Presented at the IEEE Power Electronics Specialists Conference, Orlando, FL, USA.
- [12] Almeida, P., Pereira, P., & Fino, H. (2013). Using Variable Width RF Integrated Inductors for Quality Factor Optimization. *Technological Innovation for the Internet of Things*, 394, 619–627.
- [13] Chen, J., & J. Liou, J. (2003). On-chip spiral inductors for RF applications: An overview. *Journal of Semiconductor Technology and Science*, 4(3), 149–167.

- [14] Liu, J., Shi, Y., Wen, X., Chen, D., Luo, T., Huang, H., Wang, Y. (2008). On chip spiral inductor with novel gradually changed structure. *Microwave and Optical Technology Letters*, 50(8), 2210–2213.
- [15] Sunderarajan S. Mohan, Maria del Mar Hershenson, Stephen P. Boyd, and Thomas H. Lee. (1999). Simple Accurate Expressions for Planar Spiral Inductances, *IEEE Journal Of Solid-State Circuits*, 34(10), 1419–1424.
- [16] Pirouznia, P., & Ganji, B. A. (2014). Analytical Optimization of High Performance and High Quality Factor MEMS Spiral Inductor. *Progress In Electromagnetics Research M*, 34, 171–179.
- [17] Kuo, J.-T., Su, K.-Y., Liu, T.-Y., Chen, H.-H., & Chung, S.-J. (2006). Analytical calculation for DC inductances of rectangular spiral inductors with finite metal thickness in the PEEC formulation. *IEEE Microwave and Wireless Components Letters*, 16(2), 69–71.
- [18] Musunuri, Surya, & Chapman, P. L. (2005). Design of Low Power Monolithic DC-DC Buck Converter with Integrated Inductor. Presented at the IEEE 36th Power Electronics Specialists Conference, Recife, Brazil.
- [19] Yue, C. P., & Wong, S. S. (2000). Physical modeling of spiral inductors on silicon. *IEEE Transactions on Electron Devices*, 47(3), 560–568.
- [20] Dhahri, Y., Ghedira, S., & Besbes, K. (2016). Design of an Integrated Inductor with Magnetic Core for Micro-Converter DC-DC Application. *Transactions on Electrical and Electronic Materials*, 17(6), 369–374.
- [21] Vanukuru, N. R. V., & Chakravorty, Anjan. (2014). Integrated layout optimized high-g inductors on high-resistivity SOI substrates for RF front-end modules. Presented at the International Conference on Signal Processing and Communications (SPCOM), Bangalore, India.
- [22] Mallik, K., Abuelgasim, A., Hashim, N., Ashburn, P., & Groot, C. H. d. (2014). Analytical and numerical model of spiral inductors on high resistivity silicon substrates. *Solid-State Electronics*, 93, 43–48.
- [23] Namoune, A., Taleb, R., Mansour, N., & Belboula, A. (2019). Design and modeling of integrated octagonal shape inductor with substrate silicon in a buck converter. *Indonesian Journal of Electrical Engineering and Informatics (IJEEI)*, 7(3), 527–534.
- [24] Wang, C., & Kim, N.-Y. (2012). Analytical optimization of high-performance and high-yield spiral inductor in integrated passive device technology. *Microelectronics Journal*, 43(3), 176–181.